Radar interferometry techniques for the study of ground subsidence phenomena: a review of practical issues through cases in Spain

Tomás, R.[1,2], Romero, R.[3], Mulas, J.[2,4], Marturià, J.J.[5], Mallorquí, J.J.[6], Lopez-Sanchez, J.M.[2,7], Herrera, G.[2,4], Gutiérrez, F.[8], González, P.J.[9], Fernández, J.[10], Duque S.[6], Concha-Dimas, A.[5], Cocksley, G.[11], Castañeda, C.[12], Carrasco, D.[3], Blanco, P.[13]

(1) Departamento de Ingeniería de la Construcción, Obras Públicas e Infraestructura Urbana, Escuela Politécnica Superior, Universidad de Alicante, P.O. Box 99, E-03080 Alicante, Spain. Tel. (+34) 965903400. Roberto.tomas@ua.es

(2) Unidad Asociada de investigación IGME-UA de movimientos del terreno mediante interferometría radar (UNIRAD).

(3) INDRA Espacio, Mar Egeo 4, Pol. Industrial nº 1, San Fernando de Henares, Madrid, 28830, Spain. Tel. (+34) 914805000. rromero@indra.es

(4) Geohazards Remote Sensing Laboratory, Grupo de Riesgos Geológicos, Instituto Geológico y Minero de España, Ríos Rosas 23, E-28003 Madrid, Spain. Tel. (+34) 91349 5785. j.mulas@igme.es, g.herrera@igme.es

(5) Institut Geològic de Catalunya, Balmes 209-211, Barcelona, Spain. Tel. (+34) 935538430. jmarturia@igc.cat

(6) Remote Sensing Lab., Departament de Teoria del Senyal I Comunicacions, Universitat Politècnica de Catalunya, Campus Nord Ed. D3, Jordi Girona 1-3, 08034 Barcelona, Spain. Tel. (+34) 934017229. mallorqui@tsc.upc.edu

(7) Departamento de Física, Ingeniería de Sistemas y Teoría de la Señal (DFISTS), Escuela Politécnica Superior, Universidad de Alicante, P.O. Box 99, E-03080 Alicante, Spain. Tel. (+34) 965909597. Juanma.lopez@ua.es

(8) Department of Earth Sciences, University of Zaragoza. Pedro Cerbuna 12, 50009 Zaragoza, Spain. Tel. (+34) 976761090. fgutier@unizar.es

(9) Department of Earth Sciences, University of Western Ontario, Biological & Geological Sciences Building, London, Ontario, N6A 5B7, Canada. pgonzal4@uwo.ca

(10) Institute of Geosciences (CSIC-UCM), Facultad de Ciencias Matemáticas, Plaza de Ciencias 3, 28040 Madrid, Spain. Tel. (+34) 913944632. jft@mat.ucm.es

(11) Altamira Information, Còrsega 381-387, E-08037 Barcelona, Spain. Tel. (+34) 931835750. geraint.cooksley@altamira-information.com

(12) Estación Experimental de Aula Dei (EEAD-CSIC), P.O. Box 13034, 50080 Zaragoza, Spain. Tel. (+34) 976716069. ccastaneda@eead.csic.es

(13) Institut Cartografic de Catalunya, Balmes 209-211, Barcelona, Spain. Tel. (+34) 935671500. pablo.blanco@icc.cat

Abstract

Subsidence related to multiple natural and human-induced processes affects an increasing number of areas worldwide. Although this phenomenon may involve surface deformation with 3D displacement components, negative vertical movement, either progressive or episodic, tends to dominate. Over the last decades, Differential SAR Interferometry (DInSAR) has become a very useful remote sensing tool for accurately measuring the spatial and temporal evolution of surface displacements over broad areas. This work discusses the main advantages and limitations of addressing active subsidence phenomena by means of DInSAR techniques from an end-user point of view. Special attention is paid to the spatial and temporal resolution, the precision of the measurements, and the usefulness of the data. The presented analysis is focused on

DInSAR results exploitation of various ground subsidence phenomena (groundwater withdrawal, soil compaction, mining subsidence, evaporite dissolution subsidence and volcanic deformation) with different displacement patterns in a selection of subsidence areas in Spain. Finally, a cost comparative study is performed for the different techniques applied.

Keywords: subsidence, DInSAR, settlement, remote sensing, Spain, technique-cost

1. Introduction

The term subsidence refers to the sudden sinking or gradual downward settling of the ground surface with little or no horizontal motion (Jackson 1997). Active subsidence may be related to multiple natural and anthropogenic processes (Corapcioglu 1989; Waltham 1989; Galloway et al. 1999). The risk to people and their infrastructures posed by subsidence phenomena in remote and non-inhabited areas is generally negligible. However, active subsidence in developed areas may cause significant damage to human structures, often involving multi-million dollar losses (e.g. Kappel et al. 1999; Autin 2002; Gutiérrez et al. 2009; Mancini et al. 2009). Wu (2003) points out that subsidence constitutes a hazard for bridges, roads, railways, storm drains, sewers, canals, levees, buildings and well pipes, and increases the susceptibility to tidal flooding in low-lying coastal areas. Moreover, catastrophic subsidence may result in human life lost (Guerrero et al. 2008; Galve et al. 2012). For instance, in the Far West Rand of South Africa, sudden sinkholes induced by dewatering of dolomite aquifers for gold mining have caused a total of 38 fatalities (De Bruyn and Bell 2001).

Land subsidence is the surface evidence of shallow or deep-seated deformation induced by a wide variety of natural or anthropogenic subsurface processes. Following

Prokopovich's genetic classification of subsidence (1979), endogenic subsidence is associated with internal geological processes such as faulting, folding, isostatic adjustments and volcanism. Exogenic subsidence is related to anthropogenic or natural processes involving the creation of cavities and/or the removal of material from the subsurface. The main causal mechanisms of exogenic subsidence include dissolution, degradation of organic matter, piping, thawing of ground ice, bioturbation, piezometric falls related to reduced aquifer recharge, fluid withdrawal (e.g. water, petroleum and gas), underground mining, tunnelling (Waltham 1989; Galloway et al. 1999; Gonzalez de Vallejo and Ferrer 2011).

In the pre-mitigation investigation phase, a combination of scientific understanding of these processes and a careful management can minimize the subsidence. Then, subsidence investigations are important to delineate the extent of the affected area, measuring the surface displacements (magnitude, rate and temporal and spatial variability), determining the strain mechanisms and identifying precursory/premonitory displacement indicative of potential catastrophic subsidence events in order to propose and design mitigation measures. Once mitigation measures are applied, subsidence monitoring allows evaluating the effectiveness of the adopted corrective or preventative measures, and forecasting the future behaviour of the subsidence phenomena. Numerous techniques are used for measuring and mapping spatial gradients and temporal rates of regional and local subsidence (Galloway et al. 1998; Galloway and Burbey 2011). The approaching selection is generally based on several key factors (Tomás et al. 2008; Galloway and Burbey 2011) including:

1) the cost, usually the most relevant conditioning parameter;

2) the required accuracy and resolution, conditioned by the type of subsidence phenomenon;

3) the type of data (punctual, linear, spatially distributed) and measuring frequency (time between measurement acquisitions), which are largely determined by the subsidence pattern (extent, rate, spatial and temporal variability);

4) land cover (rock outcrops, forest, urban, etc.), and weather conditions;

5) flexibility of the method, related to the possibility to selecting the time and location of the measurement acquisition, the data availability (ease of access to the data), as well as the acquisition time (time required to complete a measurement campaign); and

6) geometry and the kinematics of the subsidence phenomenon.

This paper reviews DInSAR data exploitation related to different ground subsidence phenomena (groundwater withdrawal, soil compaction, mining and evaporite dissolution subsidence and volcanic deformation) investigated in nineteen areas of Spain (Figure 1). Targeted subsidence areas differ in their extent, subsidence rates, and temporal evolution. This work highlights the main advantages and limitations of addressing the investigation of active subsidence with DInSAR techniques from an end-user point of view; i.e. spatial and temporal resolution, precision of the measurements, and utility of the data. Finally, a discussion on the cost-effectiveness of the different monitoring techniques used in Spain is presented.

Figure 1. Subsidence areas investigated by means of the Differential SAR Interferometry (DInSAR) technique in Spain and reported in this work.

2. A brief introduction to DInSAR

Synthetic Aperture Radar (SAR) and its derived techniques, like SAR interferometry (InSAR), have been widely addressed and reviewed in the scientific literature (Massonnet and Feigl 1998; Bamler and Hartl 1998; Ferretti et al. 2001; Hanssen 2001;

Crosetto et al. 2005b; Kampes 2006; Simons and Rosen 2007; Prati et al. 2010; Hooper et al. 2012). One of the main applications of SAR interferometry is the detection of Earth´s surface displacements through Differential Interferometry (DInSAR), which has shown to be a tool of great potential over the last decades. Initial single interferogram DInSAR techniques, commonly referred to as conventional DInSAR techniques, (Massonnet et al. 1993; Peltzer and Rosen 1995) evolved to advanced DInSAR techniques which provide information on the temporal evolution of the ground displacement, with a theoretical millimetric precision under favourable conditions. According to Sansosti et al. (2010), advanced DInSAR techniques can be grouped into two main categories: Persistent Scatterers (PS) methods that work on localized targets (Ferretti et al. 2001; Arnaud et al. 2003; Werner et al. 2003), and Small Baseline (SB) methods that utilize spatially distributed targets (Lundgren et al. 2001; Berardino et al. 2002; Mora et al. 2003; Schmidt and Bürgmann 2003; Prati et al. 2010). Such techniques have been applied to ground displacements related to active tectonics, seismic events, volcanism, anthropogenic subsidence and uplift, landsliding or glacier dynamics.

The basic concept of the DInSAR techniques is to monitor an area through time on a regular basis. The SAR images acquired in different dates are then combined in pairs to generate a set of differential interferograms that contain information on the interferometric phase (ψ_{int}). Ideally, differential interferograms should contain only the ground displacement component between the acquisition times of the two SAR images. However, in practice, there are other terms contributing to the interferometric phase that can mask the desired ground displacement information, e.g. phase contributions from atmospheric water vapour (ψ_{atmos}). The goal of the different processing techniques is to accurately isolating the displacement term from the remaining components. The interferometric phase can be expressed as the sum of the following terms (Hanssen 2001):

$$\psi_{\text{int}} = \psi_{flat} + \psi_{topo} + \psi_{mov} + \psi_{atmos} + \psi_{noise} \qquad (1)$$

where ψ_{flat} is the flat-earth component related to range distance differences in absence of topography, ψ_{topo} is the topographic phase, ψ_{mov} is the phase contribution due to ground displacement occurring between the two SAR image acquisitions, measured along the line of sight (LOS), ψ_{atmos} is the phase component due to atmospheric disturbances or artefacts, and ψ_{noise} includes the remaining noise sources. The first two terms in (1) can be expressed analytically and ψ_{topo} can be extracted from an independent DEM.

The degradation of the quality of the interferometric phase (decorrelation) has a non-uniform impact on the interferograms. Depending on several factors like the land cover, presence of human structures, surface changes due to human or natural activity, some areas may have a better quality phase. Consequently, a selection of the more reliable pixels from a set of interferograms has to be performed. The pixel selection criterion can be established based on the estimation of their phase quality using two different approaches: the *coherence stability* and the *amplitude dispersion*. For the former, a multi-looked pixel is selected if it presents coherence values higher than an established threshold in a certain percentage of interferograms (Berardino et al. 2002; Mora et al. 2003). For the latter, the phase standard deviation of each pixel is assumed to be related to its temporal radar signal amplitude stability (low dispersion) and selected if it exceeds a certain threshold (Ferretti et al. 2001). The selection criterion determines the nature of the targets to work with. While the amplitude dispersion selects ideal point-like targets at the maximum spatial resolution of the SAR image, the coherence stability implies an averaging of a set of pixels, leading to a lower spatial resolution product.

Depending on the setting, it may be necessary to decrease the number of selected points by employing a coherence approach, rather than having the maximum spatial resolution information provided by the amplitude approach. For instance, in volcanic areas where rock outcrops have large extent and temporal stability, the coherence-based processing is generally more appropriate. In contrast, in urban areas where man-made targets are more likely to be found, the amplitude-based processing is typically better suited. Another decisive issue is the number of available images. A reliable relationship between amplitude and phase stability cannot be obtained with a limited number of images. On the other hand, the coherence estimator is more robust when dealing with a low number of interferograms. Considering both criteria, a compromise between the number of pixels selected and their reliability should be found.

For measuring ground displacement, satellite-based DInSAR techniques present three immediate advantages compared to classical ground-based methods such as the Differential Global Positioning System (DGPS): low-cost, measurement repetitiveness and availability of historical data. Firstly, they provide, at a low cost, displacement measurements across wide areas and with a high spatial density, as opposed to the discrete point data supplied by instrumental techniques, restricted to benchmarks with a much lower density and generally covering smaller areas. For instance, the widely used SAR images acquired by the European ERS or ENVISAT and the German TerraSAR-X satellites cover an area of 100 km by 100 km and 30 km by 50 km respectively. Secondly, orbital sensors have a short revisiting time period, which makes it possible to monitor at selected locations with a high frequency. Thirdly, the low incidence angle (i.e. the angle between the satellite line-of-sight (LOS) and a line perpendicular to the land surface) makes InSAR technique very sensitive to vertical displacements produced by subsidence. Finally, the relatively long archive of SAR images acquired since 1992 allows studying, at least in Europe, almost any area since that date. Nevertheless, DInSAR techniques should be considered as complementary, rather than a complete replacement of the ground-based techniques.

3. Advantages and limitations of DInSAR from the end-user point of view

In the last 20 years the importance of DInSAR as a subsidence monitoring tool has increased significantly. In Spain, nineteen areas affected by active subsidence have been studied using different DInSAR techniques. These studies exploit radar data from seven sensors, which include satellite- and ground-based (Tables 1 and 2). These case studies deal with subsidence due to groundwater withdrawal, mining activity, volcanism, impoundment of water reservoir, evaporite dissolution, and the superposition of some of the above mentioned processes. Although most of these subsidence cases were previously known and characterized, the application of DInSAR techniques allowed gaining greater insight into the deformation patterns, specially providing quantitative strain data. In this section, the main advantages and limitations of the DInSAR techniques from an end-user point of view are discussed and illustrated through subsidence case studies from Spain.

Table 1. Radar systems employed in the reported subsidence studies in Spain. ESA: European Space Agency; DLR: German Aerospace Center; JAXA: Japan Aerospace Exploration Agency; UPC: Universidad Politécnica de Cataluña; ASI: Italian Space Agency.

Table 2. DInSAR technique and pixel selection criteria implemented in the software packages applied to study subsidence in Spain. Software developer is also indicated.

3.1 Spatial resolution

The spatial resolution of DInSAR data is crucial in subsidence studies with an applied objective. The spatial resolution of the ground displacement data depends on the radar sensor and the processing algorithm. The pixel selection methods based on amplitude criteria allow keeping the original resolution of the SAR image. On the other hand, by definition, coherence selection techniques involve an averaging of adjacent pixels of the original image with the consequent degradation in spatial resolution. Using the coherence approach, typical resolutions of DInSAR maps obtained from ERS and ENVISAT data are 60 m × 60 m, 80 m × 80 m and 100 m × 100 m. These values correspond to the multilook averaging of 3 × 15, 4 × 20, and 5 × 25 pixels in azimuth and range respectively. Spatially restricted subsidence phenomena, such as those related to evaporite dissolution-induced sinkholes in the *Ebro Valley* (Castañeda et al. 2009b) or a salt mine below *Sallent* village (López et al. 2010), usually affect areas smaller than 1 km^2. Consequently, they require an appropriate compromise between resolution and electromagnetic response stability. As an example, the 80-m pixel-sized DInSAR map of Figure 2 provides partial displacement data on a subsidence basin induced by underground mining but does not allow analysing subsidence at a building scale (Herrera et al. 2012). DInSAR applications for built areas and infrastructures require very high resolutions in order to obtain information on individual buildings or elements of a structure rather than an averaged subsidence rate for an area including several constructions. For *Murcia* city (Figure 3), Herrera et al. (2009b) demonstrated that amplitude techniques, which work at full resolution, provide a higher density of reliable points than coherence based techniques. Moreover, using different bands TSX has demonstrated to provide the highest PSs density (Crosetto et al. 2010; Herrera et al.

2010). Figure 3 shows that the X-band based PSs density is at least ten times higher than the PSs density provided by C-band satellites (Herrera et al. 2010).

Figure 2. Detail of the 80-m pixel-sized DInSAR map of mining subsidence in La Unión for the period 2005-2008. Grey line corresponds to the 1:5000 topographic map.

Figure 3. DInSAR maps showing subsidence rates caused by aquifer overexploitation in the *Vega Media of the Segura River* (Spain) obtained from images acquired by different sensors and for three successive of time periods: a) 1995-2005 period (ERS and ENVISAT sensors). b) 2005-2008 period (ENVISAT sensor). c) 2008-2009 period (TerraSAR-X sensor). d) Temporal evolution of the subsidence from 1995 to 2009, plotted alongside the variations in the piezometric level. Syr^{-1} is the average number of SAR images per year, and *dgp* is the existing maximum temporal gap (expressed in days) between two SAR images.

3.2 Temporal resolution

The temporal resolution of the ground displacement data depends on the satellite revisiting period (Table 1) that determines the availability of SAR images of the study area. Consequently, generally the shorter the revisiting time the more accurate may be the analysis of the temporal evolution of the subsidence phenomenon. In areas with high subsidence rates the revisiting period should be as short as possible in order to avoid aliasing problems. Aliasing is introduced when the sampling frequency is too low and ~~affects~~ the motion of ground targets or pixels with LOS displacement between the two dates under study is greater than the system resolution; i.e. half the radar wavelength (λ/2). Moreover, shorter revisiting periods improve the ability to identify non-linear or seasonal displacement patterns. COSMO SkyMed and TerraSAR-X, with the shortest revisiting periods (Table 1), are more appropriate systems to study non-linear and episodic subsidence phenomena than e.g. ALOS-PALSAR with longer revisiting periods, although they are more prone to temporal decorrelation in non-urban areas due to their sensitivity of phase values to any change in scatterers distribution (Prati et al. 2010). As an example, *La Unión* area (Figure 4) exhibits significant gaps of displacement information due to high deformation rates (4.8 cm per month) related to mining subsidence (Herrera et al. 2007).

The acquisition time of terrestrial sensors (Ground based SAR- GBSAR), which is selected by the user, allows to define the time between successive acquisitions as much as few minutes. However, although radar sensors can be strategically placed in prominent locations in order to get an optimal LOS they are generally limited by the high incidence angle (Pipia et al. 2007; 2008; Monserrat 2012). ERS and ENVISAT satellites provide a long historical archive of radar data for almost all the Spanish territory between 1992 and 2012 with a gap during 1994, allowing to retrospectively processing data in areas where ground-based data is lacking. Historical data are necessary for the long-term monitoring of areas with low subsidence rate and for the application of advanced DInSAR techniques which require a large number of images. In contrast, TerraSAR-X data is limited to the areas where acquisitions have been previously requested; i.e. on-demand system. The same applies to GB-SAR, since also data availability is limited to planned images in monitored areas.

Another important issue for DInSAR subsidence analysis is the sensor wavelength (λ). Most studies reviewed in this work are based on C-band sensors due to high data availability. However, DInSAR based on C-band radar data is frequently limited due to the incoherence/decorrelation related to the land covers. In this sense, in *Sant Quirte del*

Valles (see location in Figure 1), Blanco et al. (2008) observed that L band–based DInSAR (λ = 23 cm) provides coherent information where C band–based DInSAR (λ = 5.6 cm) measurements are predominantly incoherent showing that a significant part of the backscattered echo arrives from the ground rather than from vegetation in agreement with other authors (Colesanti and Wasowski 2006; e.g. Raucoules et al. 2007; Hooper et al. 2012) .

Figure 4. Detail of C-band DInSAR map of *La Unión,* showing the effect of aliasing on the availability of Persistent Scatterers due to ~~for~~ high subsidence rates related to mining. The lack of colored pixels (displacement data) in the urban area of *Lo Tacón* is due to the loss of coherence. Levelling isolines indicates cumulative displacement in cm during the time period 1998-2000 and show a displacement rate~~s~~ higher than 40 mm/year (Rodríguez-Estrella et al. 2000).

3.3 Influence of the terrain characteristics on persistent scatterers detection

The backscattering of the microwave signals depends on the characteristics of the terrain and the weather conditions at the acquisition time. Generally, vegetated areas and water bodies disperse the radar emitted SAR signals, reducing the amount of returned signal to the satellite (Ulaby et al. 1982; Henderson and Lewis 1998). In some areas the changes in the vegetation between two radar acquisitions can produce such a significant loss of coherence that the displacement information is almost impossible to obtain. On the contrary urban areas, or rock outcrops provide a stable electromagnetic response through time, being considered more suitable for applying DInSAR techniques. This circumstance is illustrated by studies carried out in the subsidence areas of Orihuela village (Tomás et al. 2007; 2010b), where PS densities from 0 to 10

PS per km^2 have been obtained in rural areas, whereas more than 100 PS per km^2 were obtained in urbanized areas and zones dominated by rock outcrops (Figure 5). Rocky areas like the *Tenerife* Island and urban scenarios such as *Murcia* city, *Orihuela* village or *Sallent* village provide a high amount of PS points. However, the proportion of PS points is reduced considerably in the agricultural areas of *Vega Media and Baja of the Segura River* (Herrera et al. 2009b; Tomás et al. 2010b), *Granada* basin (Fernandez et al. 2009; Sousa et al. 2010) and the *Ebro* valley (Castañeda et al. 2009b) (see Figure 1 for locations).

The weather conditions also affect the transmission of the microwaves producing atmospheric artefacts which may limit the use of DInSAR techniques. Variations in water vapour, temperature, and pressure along the distance travelled by the signal within the atmosphere can produce a delay in the transmission of the microwaves affecting the interferometric phase and distorting the phase related to the actual ground displacement. This fact has been observed in the *Ebro* valley (Figure 6), where a significant proportion of the interferograms was affected by atmospheric artefacts (Castañeda et al. 2011).

Figure 5. Detail of DInSAR map based on the Coherent Pixel Technique (CPT) showing the water withdrawal induced subsidence measured along the LOS in the city of *Orihuela* and surrounding areas from 1993 to 2009. Note the high and a low density of PSs in the urban/rocky and agricultural areas, respectively. The lack of PSs in the SE slope of the mountain is related to its non-favorable orientation with respect to that of the LOS.

Figure 6. a) Location of three areas ~~areas~~ affected by active ground deformation in the Ebro Valley analysed using conventional (interferograms) and SBAS techniques. b)

Mixed urban-agricultural area with active sinkholes related to evaporite dissolution in a mantled karst setting. c) Mixed agricultural and natural vegetated area showing active landslides in a gypsum escarpment affected by river undercutting. d) Area with natural xerophytic vegetation showing subsidence induced by salt room and pillar mining. On the numbers on the left images, indicate subsidence rates measured using SBAS. In the central images, every color fringe corresponds to a 2π phase change (2.6 cm). The plots show displacement time series for selected points (highlighted in green) from 1995 to 2000.

3.4 Type of results

Generally, DInSAR provides a great deal of information on subsidence distribution, magnitude and kinematics, as well as on the processing quality. These data, measured along satellite LOS, are generally represented as maps that show the displacement spatial distribution, either average rate or accumulated magnitude. The former corresponds to the average displacement rate for the considered period of time, expressed in mm/year or cm/year (e.g. Figure 4), whereas the latter is the total amount of subsidence with respect to the first SAR acquisition, usually expressed in mm or cm (e.g. Figures 2 and 4). When conventional interferometry is used, the results can be also depicted using fringes that represent a 2π phase change (Figure 6), which corresponds to a displacement of $\lambda/4\pi$ meters, where λ is the wavelength (in meters) of the microwave used by satellite. Note that ALOS-PALSAR satellite (L-band) has a wavelength of 23.6 cm whilst TerraSAR-X or Cosmo-Skymed-1 satellites (X-band) have a wavelength of 3.1 cm (Table 1). As a consequence, it can be stated that L-band satellite is less sensitive to the displacement (one fringe corresponds to 11.8 cm instead of the 1.6 cm of X-band satellites).

The temporal evolution of subsidence for a given point can be represented when a set of images is used in the processing. Therefore, for every radar measurement we provide: (1) the position of the PS: three geographical coordinates and (2) the temporal evolution of the displacement over the processed/analysed time period (e.g. Figure 3d).

3.5 Applications of DInSAR information

A close cooperation between DInSAR specialists and end-users (geoscientists, civil engineers, land-use planners, Civil Protection Authorities, insurance companies, etc.) is necessary in order to fully exploit the high capability and practicality of these remote sensing techniques. In *Spain*, DInSAR has been used for the monitoring of known subsiding areas, providing spatially denser displacement information of the area of interest than ground-based techniques. However, one of the most interesting applications of these interferometric techniques is the early detection of unknown ground motion (e.g. Crosetto et al. 2005a; Mora et al. 2007; Castañeda et al. 2009a; Castañeda et al. 2009b; Fernandez et al. 2009; González et al. 2010; González and Fernández 2011a; Pulido-Bosch et al. 2011). Some Spanish institutions, such as the Institut Geologic de Catalunya, IGC, (Mora et al. 2007) have periodically and systematically monitored wide geographical areas in order to recognize areas affected by subsidence or other ground instability processes in *Catalonia*. The *Geological Hazard Prevention Map of Catalonia* (MPRGC 1:25000) includes the DInSAR information. This open-accesses cartographic database allows the public to consult, via the IGC, ground displacement results (Oller et al. 2011).

Another interesting application of DInSAR in Spain is the incorporation of ground displacement data in the development of susceptibility and risk maps. In *Sallent* village, severely affected by subsidence due to salt mining, DInSAR data has been integrated into a Geographical Information System (GIS) together with abundant spatial data (geological, geotechnical, geophysical, topographic levelling, extensometer and inclinometer measurements, etc.) in order to analyse and manage different scale spatial data for risk analysis and mitigation (Marturià et al. 2006; Palà et al. 2006; Marturia et al. 2010). Subsidence modelling, aimed at reproducing and/or predicting displacements under certain conditions, is generally a complicated task. In Spain, DInSAR has shown to be a useful tool for calibrating and validating subsidence models. In Murcia city, affected by subsidence due groundwater withdrawal and aquitard consolidation (Mulas et al. 2003), InSAR data have been used to validate numerical geotechnical models (Herrera et al. 2009a) and to calibrate hydrological models that predict future scenarios of piezometric level change (Tomás et al. 2010a) (Figure 7). DInSAR data, jointly with in-situ measurements (piezometric level and geological-geotechnical information), are being used by the *Vega Baja and Media* of the *Segura* river local authorities for water supply management. In *Sallent*, the geometry of mining and karstic cavities in a salt formation have been modelled to match topographic levelling (López et al. 2010). In the *Sant Feliu del Llobregat* pilot site, water extraction volumes have been incorporated into geological models to match DInSAR data with water pumping points and volumes (Concha et al. 2010). In *Murcia* and *Orihuela* DInSAR data have been used for building damage mapping (Herrera et al. 2010; Bru et al. 2013; Herrera et al. 2012; Tomás et al. 2012) (Figure 8). DInSAR displacement measurements have also allowed the identification of damage on buildings and other man-made structures (bridges, sidewalks, walls, etc.). This application has been substantially improved since the launch of the TerraSAR-X satellite that provides a high spatial resolution and allows computing the angular distortions and the differential settlement affecting the individual buildings.

Recent works (Tomás et al. 2010b; Tomás et al. 2011) have analysed the influence of different triggering and conditioning factors on subsidence phenomena by integrating DInSAR data from the *Segura* River valley with multiple variables in a GIS environment. The cross analysis of the different factors and the subsidence maps reveals some interesting relationships between the different factors that influence subsidence. These findings can be used as the basis for the hydraulic management of the watershed.

Figure 7. Modelling of subsidence caused by groundwater withdrawal in *Murcia* city. The model has been calibrated using InSAR data for the period 1993-1995 and extrapolated for 1995-2007.

Figure 8. Detail of DInSAR map of *Murcia* city applied for building damage monitoring. Above: Subsidence rates measured from 1995 to 2008 (left) and from 2006 to 2010 (right). Center: Cross-section depicting the surface damage observed in three adjacent buildings with different foundations along the transect X-X' indicated in the detailed DInSAR map. Below: Profile of the subsidence magnitude recorded along X-X'.

Studies conducted in the *Canary Islands* (Fernández et al. 2002; Fernández et al. 2003; Fernández et al. 2005; Fernández et al. 2009; González et al. 2010; González and

Fernández 2011b) have shown that DInSAR is a very powerful technique for the volcano activity monitoring in an operative and systematic way.

Polarimetric SAR Interferometry (PolInSAR) has been recently used by several researchers (Navarro-Sanchez et al. 2010; Navarro-Sanchez and Lopez-Sanchez 2012) in order to increase the number of PS candidates. This approach allows increasing the PS density by the identification of pixels with good phase quality after a search in the available polarimetric space.

3.6 Independent validation of the DInSAR results: measurements precision

Strong efforts have been done in order to assess independently the precision of the DInSAR subsidence measurements. This independent validation process is usually performed by comparing DInSAR data with in situ measurements. Consequently, in situ displacements have to be projected along the LOS in order to be able to make direct comparisons. The precision of DInSAR techniques, defined as the dispersion of the displacement estimates around the expected value, depends on a number of parameters (e.g. González and Fernández 2011b; Hooper et al. 2012) whose exposition is out of the scope of this work. However, some authors (Colesanti and Wasowski 2006; Lanari et al. 2007; Raucoules et al. 2007; Prati et al. 2010; e.g. Ferretti et al. 2011; Hooper et al. 2012) suggested a typical precision for average displacement rate and LOS displacements values of up to ±1mm/year and ±5 mm respectively. So far, the direct comparison of DInSAR subsidence data with displacement values measured in situ is the most common way to evaluate the precision of these techniques. Some subsidence areas in Spain monitored with DInSAR have been compared with geodetic or topographical measurements (e.g. Tenerife Island; Fernández et al. 2003; 2009) resulting in good sub-centimetre agreements (Figure 9). Table 3 shows the precisions of DInSAR measurements obtained by several authors.

Figure 9. (a) Comparison of subsidence measurements in Tenerife Island obtained by Small Baseline InSAR and GPS. The GPS values have been projected along the LOS for direct comparison. (b) Location of the comparison points, color-coded according to the correlation index between the time series of displacements from the two techniques.

Table 3. Estimated precision of subsidence measurements obtained with DInSAR in the analysed areas of Spain (See Figure 1 for locations). (*) The error is computed as the average absolute difference between the in situ and InSAR measurements for the whole available data.

4 Cost analysis of InSAR

A comparative summary of the different techniques most frequently used for measuring subsidence is presented in Table 4. The characteristics summarized for each technique include accuracy, displacement component, survey scale, conditions and characteristics of the operating environments, degree of automation and sampling frequency. A detailed description of some of these techniques employed for subsidence monitoring can be found in Galloway (1998) and Galloway and Burbey (2011).

Table 4. Comparative of method for measuring ground subsidence. G: Good; MD: Medium; P: Poor; MN: Manually; A: Automatic; SA: Semiautomatic.

A comparative study of the eight techniques used for monitoring the subsidence in 11 case studies in Spain was performed for estimating their cost. Monitoring parameters not considered in Table 4, such as the temporal frequency of the measurements (time interval between consecutive measurements) and the mapped point density (number of measurements per unit area), were also included. The evaluation of the cost for the different techniques (levelling, InSAR, GPS, etc.) is heterogeneous because of the distinct operational context. For this reason we assume a similar post-processing cost for the different techniques. Therefore, the cost calculation is based on the commercial (non-scientific) SAR image price or the value of every field campaign. In the case of the geodetic station of *Lanzarote* and the automatic extensometer of *Sallent*, the value has been computed considering the annual maintenance cost of these instruments.

The following economic parameters have been estimated: (a) the annual cost per measurement point; (b) the difference between the annual costs of each approach and the cost using ERS-ENVISAT-based InSAR. This parameter provides an idea about how costly or inexpensive are the considered techniques in comparison with InSAR ERS-ENVISAT processing through a year; (c) the annual cost per unit area (km^2) with respect to ERS-ENVISAT-based InSAR processing; and (d) the annual cost per measurement point relative to the price estimated for monitoring the same point by means of ERS-ENVISAT images. For all of them, the maximum, minimum and mean values have been computed.

The results of the analysis are shown in Figure 10. Figure 10a shows the mean measurement frequency (per year) of eight techniques considered. The acquisition frequency is crucial for identifying and analysing subsidence phenomena with non-linear or episodic kinematics. Excluding the continuous acquisition systems that are usually installed in areas affected by rapid subsidence and where a high risk for population exists, the highest measurement frequencies correspond to CosmoSkyMed (up to 15 possible measurements per year) and TerraSAR-X (8.7 - 21.6 measurements per year). ERS-ENVISAT processings provide between 6 and 10 measurements per year. Usually, levelling, GPS and extensometers are used for providing 1 or 2 measurements per year.

The point density (number of points with subsidence measurement per square kilometre) is critical for identifying the spatial subsidence patterns (Figure 10b). The highest point density is provided by the TerraSAR-X satellite (average, minimum and maximum density of 825, 701 and 916 points per square kilometre, respectively) due to its high resolution. CosmoSkyMed and the automatic total stations also provide a high point density. However, the latter has the disadvantage of measuring benchmarks located at short distances (< 1 km). Levelling and ERS-ENVISAT InSAR provide a similar point density, with mean values of 93 and 51 points per square kilometre, respectively. GPS, extensometer and geodetic stations provides the lowest density of subsidence measurements, with maximum values of 4 points per square kilometre. The geodetic station has been included in the cost analysis. It is a singular laboratory located under exceptional environmental conditions which includes high-precision geodetic instrumentation (e.g., tiltmeters, strainmeters, gravimeters, GPS, etc.) with continuous acquisition data systems. The geodetic station is not only used to carry out the study of the geodynamics processes but also the instrumental research. As example, the geodetic station located in Lanzarote Island (Vieira et al. 1991; Fernández et al. 1992) includes three instrumental locations dedicated to the study of the Solid Earth deformations, Earth Tides, sea-level variations, etc.

A relevant parameter from the economic feasibility perspective is the annual cost per point, given by the ratio between the total annual cost of the implementation of the technique in Euros, and the available number of information points. The results show that the four case studies analysed by means of TSX-InSAR provide the lowest annual cost (0.65 € per year per point) in comparison with the average cost of the eleven cases analyzed with ERS-ENVISAT-InSAR (1.20 € per year and point), and the remaining techniques (Figure 10c). Levelling, extensometers and GPS have the highest prices per measurement point and year, ranging from 220 to 1007 Euros. Figure 10f shows the annual cost per measurement point compared with InSAR. Although TSX-InSAR provides the lowest mean cost per point (Figure 10c), the relative cost per point is lower for the three case studies where both sensors (ERS-ENVISAT and TSX) were used.

The annual costs of the different techniques has been also computed and compared with that of the ERS-ENVISAT-InSAR (Figure 10d). Obviously, this cost strongly depends on the number of measurements obtained each year, especially for instrumental techniques (extensometers and levelling) and for GPS. For this reason, the extensometers installed over a salt mine in *Sallent, Barcelona*, which provide a continuous record (8,760 measurements per year) have not been considered in the analyses. The results show that most of the techniques considered are from 4 to 10 times more expensive than ERS-ENVISAT-InSAR. However, TSX-InSAR and GPS provides the highest mean annual costs (22 and 26 times higher, respectively).

Figure 10e shows the annual cost per square kilometre of each technique compared with that of ERS-ENVISAT-InSAR. These estimates depend to a large extent on the area extent surveyed. The InSAR techniques yield the lowest annual cost per square kilometre, in addition to their high point density, as mentioned above. The geodetic stations provide a low cost (6 times higher than ERS-ENVISAT-InSAR) because the whole Lanzarote Island (845 km^2) is monitored with only 3 measurement points. Consequently, in this case, although the annual cost unit per square kilometre is low, the spatial density of data is very poor. Due to the coverage of SAR images (100×100, 30×50 and 20×20 km for ERS-ENVISAT, TSX and CosmoSkyMed, respectively), DInSAR techniques are considered of low-cost for large study areas.

Figure 10. Comparative cost analysis of the eight techniques used for measuring the subsidence in Spain. See explanation in the text. (*) The continuous record of the extensometer installed in *Sallent* has not been considered for mean estimation. (**) The measuring network extends partially within the area with DInSAR detected movements and it has set focusing in areas with detected intensive subsidence.

5 Concluding remarks

Since the first application of DInSAR to identify soil swelling (Gabriel et al. 1989), this useful technique has become a widespread tool for subsidence monitoring, providing a high amount of ground displacement data for wide areas and at low cost compared with ground-based techniques. Nineteen subsidence areas (mining, groundwater withdrawal, evaporite dissolution, volcanism and load-induced compaction) in Spain have been recognized and/or studied using DInSAR techniques during the last twenty years. In some cases, DInSAR has allowed the identification of previously unknown subsidence areas providing information on distribution and rate of the settlement process. In other cases, DInSAR has been used as a tool for the analysis, modelling and management of potentially hazardous subsidence processes in combination with other complementary information. The principal limitations of DInSAR techniques are the loss of coherence between two acquisitions caused by temporal decorrelation (especially in agricultural and vegetated areas), the atmospheric artefacts that affect the displacement estimation,

the availability of images that depends on the satellites repeat-orbit cycle, and the low capability to measure horizontal displacements. However, the main advantages of DInSAR are the high performance measuring vertical displacements, the low cost in comparison with other techniques especially when studying large areas, the short revisiting period compared to field techniques, the large spatial coverage, the ability to operate even at night or under adverse weather conditions, and the possibility of analysing areas retrospectively using historical data since 1992 using the ESA's SAR archives. The cost analysis performed has allowed us to identify the strongest points of the InSAR techniques compared with other conventional techniques: (1) higher data acquisition frequency and spatial coverage; and (2) lower annual cost per measurement point and per square kilometre. The obtained results show that in many cases the clear advantages of DInSAR compensate and even get over the limitations of this technique.
In Spain more than ten different DInSAR techniques have been used for the study of subsidence phenomena. Although advanced techniques are widely used due to their capability to minimize atmospheric artefacts, in some cases, conventional DInSAR techniques are required due to the high velocity of the subsidence. As a consequence, DInSAR has become an indispensable tool to satisfactorily address many subsidence studies. In the future, the development of new algorithms, the launch of new satellites, the integration InSAR data with ground-based measurements and the joint performance of ground and airborne platforms will allow improving substantially the resolution and precision of DInSAR techniques and the monitoring and managing of ground subsidence hazards.

Acknowledgements

Authors thank O. Monserrat and M. Crosetto (Institut de Geomàtica) for their useful comments and the review of first version of the manuscript. The ERS and ENVISAT images mentioned in this work were provided by the European Space Agency (ESA) in the framework of the EO Cat.1-2494 and Cat.1-3462 projects and the Terrafirma GMES Project. The TerraSAR-X images were provided by DLR in the framework of the scientific project GEO0389. The different research areas included in this paper has been supported by the projects: CGL2005-05500-C02, CGL2008-06426-C01-01/BTE, AYA2010-17448, IPT-2011-1234-310000, TEC-2008-06764, ACOMP/2010/082, AGL2009-08931/AGR, 2012GA-LC-036, 2003-03-4.3-I-014, CGL2006-05415, BEST-2011/225, CGL2010-16775, TEC2011-28201, 2012GA-LC-021 and the Banting Postdoctoral Fellowship to PJG. This research is a contribution of the Moncloa Campus of International Excellence (UCM-UPM, CSIC).

References

Arnaud A, Adam N, Hanssen R, Inglada J, Duro J, Closa J, Eineder M ASAR ERS interferometric phase continuity. In: Geoscience and Remote Sensing Symposium, 2003. IGARSS '03. Proceedings. 2003 IEEE International, 21-25 July 2003 2003. pp 1133-1135 vol.1132. doi:10.1109/igarss.2003.1294035

Autin WJ (2002) Landscape evolution of the Five Islands of south Louisiana: scientific policy and salt dome utilization and management. Geomorphology 47 (2–4):227-244. doi:10.1016/s0169-555x(02)00086-7

Bamler R, Hartl P (1998) Synthetic aperture radar interferometry. Inverse Problems 14 (4):R1

Berardino P, Fornaro G, Lanari R, Sansosti E (2002) A new algorithm for surface deformation monitoring based on small baseline differential SAR interferograms. Geoscience and Remote Sensing, IEEE Transactions on 40 (11):2375-2383. doi:10.1109/tgrs.2002.803792

Blanco P, Arbiol R, Palà V (2008) ALOS-PALSAR performances on a multiple sensor DInSAR scenario for deformation monitoring applications. Paper presented at the ALOS 2008 Symposium, Rhodes, Greece, 3-7 November

Bru G, Herrera G, Tomás R, Duro J, De la Vega R, Mulas J (2013) Control of deformation of buildings affected by subsidence using persistent scatterer interferometry. Structure and Infrastructure Engineering 9:188-200. doi:10.1080/15732479.2010.519710

Castañeda C, Gutiérrez F, Galve JP, Pourthié N, Souyris JC, Manunta M (2009a) Comparación de dos técnicas de interferometría radar mediante deformaciones generadas por disolución de evaporitas, minería y deslizamientos (Valle del Ebro, España). In: Montesinos S, Fernández L (eds) Teledetección: agua y desarrollo sostenible. Zaragoza, Spain, pp 261-264

Castañeda C, Gutiérrez F, Manunta M, Galve JP (2009b) DInSAR measurements of ground deformation by sinkholes, mining subsidence, and landslides, Ebro River, Spain. Earth Surface Processes and Landforms 34 (11):1562-1574. doi:10.1002/esp.1848

Castañeda C, Pourthie´ N, Souyris J-C (2011) Dedicated SAR interferometric analysis to detect subtle deformation in evaporite areas around Zaragoza, NE Spain. International Journal of Remote Sensing 32 (7):1861-1884. doi:10.1080/01431161003631584

Colesanti C, Wasowski J (2006) Investigating landslides with space-borne Synthetic Aperture Radar (SAR) interferometry. Engineering Geology 88 (3–4):173-199. doi:10.1016/j.enggeo.2006.09.013

Concha A, Ripoll J, Piña J, Gabàs A, Piña E (2010) Two-dimensional coupled numerical modelling of subsidence due to water extraction at the Lower Llobregat River, Spain. Paper presented at the Land Subsidence, Associated Hazards and the Role of Natural Resources Development. Proceedings of EISOLS 2010, Querétaro, Mexico,

Corapcioglu MY (1989) Land subsidence a state of the art review. In: Bear M, Corapcioglu MY (eds) Fundamentals of Transport Phenomena in Porous Media. Nato, A.S.I. Series. Martinus Nijhott Publishers, Dordrecht, Netherlands, pp 369-444

Crosetto M, Crippa B, Biescas E (2005a) Early detection and in-depth analysis of deformation phenomena by radar interferometry. Engineering Geology 79 (1–2):81-91. doi:10.1016/j.enggeo.2004.10.016

Crosetto M, Crippa B, Biescas E, Monserrat O, Agudo M, Fernández P (2005b) Land deformation monitoring using SAR interferometry: State-of-the-art. Photogrammetrie, Fernerkundung, Geoinformation 6:497-510

Crosetto M, Monserrat O, Iglesias R, Crippa B (2010) Persistent Scatterer Interferometry: potential, limits and initial C- and X-band comparison. Photogrammetric Engineering and Remote Sensing 76 (9):9

De Bruyn IA, Bell FG (2001) The occurrence of sinkholes and subsidence depressions in the far west Rand and Gauteng Province, South Africa, and their engineering implications. Environmental & Engineering Geoscience 7 (3):281-295. doi:10.2113/gseegeosci.7.3.281

Fernández J, Romero R, Carrasco D, Luzón F, Araña V (2002) InSAR volcano and seismic monitoring in Spain. Results for the period 1992–2000 and possible interpretations. Optics and Lasers in Engineering 37 (2–3):285-297. doi:10.1016/s0143-8166(01)00085-9

Fernández J, Romero R, Carrasco D, Tiampo KF, Rodríguez-Velasco G, Aparicio A, Araña V, González-Matesanz FJ (2005) Detection of displacements on Tenerife Island, Canaries, using radar interferometry. Geophysical Journal International 160 (1):33-45. doi:10.1111/j.1365-246X.2005.02487.x

Fernández J, Tizzani P, Manzo M, Borgia A, González PJ, Martí J, Pepe A, Camacho AG, Casu F, Berardino P, Prieto JF, Lanari R (2009) Gravity-driven deformation of Tenerife measured by InSAR time series analysis. Geophys Res Lett 36 (4):L04306. doi:10.1029/2008gl036920

Fernández J, Vieira R, Díez JL, Toro C (1992) Investigations on crustal thickness, heat flow and gravity tide relationship in Lanzarote Island. Physics of the Earth and Planetary Interiors 74 (3-4):10. doi:10.1016/0031-9201(92)90010-S

Fernández J, Yu TT, Rodríguez-Velasco G, González-Matesanz J, Romero R, Rodríguez G, Quirós R, Dalda A, Aparicio A, Blanco MJ (2003) New geodetic monitoring system in the volcanic island of Tenerife, Canaries, Spain. Combination of InSAR and GPS techniques. Journal of Volcanology and Geothermal Research 124 (3–4):241-253. doi:10.1016/s0377-0273(03)00073-8

Fernandez P, Irigaray C, Jimenez J, El Hamdouni R, Crosetto M, Monserrat O, Chacon J (2009) First delimitation of areas affected by ground deformations in the Guadalfeo River Valley and Granada metropolitan area (Spain) using the DInSAR technique. Engineering Geology 105 (1–2):84-101. doi:10.1016/j.enggeo.2008.12.005

Ferretti A, Prati C, Rocca F (2001) Permanent scatterers in SAR interferometry. Geoscience and Remote Sensing, IEEE Transactions on 39 (1):8-20. doi:10.1109/36.898661

Ferretti A, Tamburini A, Novali F, Fumagalli A, Falorni G, Rucci A (2011) Impact of high resolution radar imagery on reservoir monitoring. Energy Procedia 4 (0):3465-3471. doi:10.1016/j.egypro.2011.02.272

Gabriel AK, Goldstein RM, Zebker HA (1989) Mapping Small Elevation Changes Over Large Areas: Differential Radar Interferometry. J Geophys Res 94 (B7):9183-9191. doi:10.1029/JB094iB07p09183

Galve JP, Gutiérrez F, Guerrero J, Alonso J, Diego I (2012) Optimizing the application of geosynthetics to roads in sinkhole-prone areas on the basis of hazard models and cost-benefit analyses. Geotextiles and Geomembranes 34 (0):80-92. doi:10.1016/j.geotexmem.2012.02.010

Galloway D, Burbey T (2011) Review: Regional land subsidence accompanying groundwater extraction. Hydrogeology Journal 19 (8):1459-1486. doi:10.1007/s10040-011-0775-5

Galloway DL, Hudnut KW, Ingebritsen SE, Phillips SP, Peltzer G, Rogez F, Rosen PA (1998) Detection of aquifer system compaction and land subsidence using interferometric synthetic aperture radar, Antelope Valley, Mojave Desert, California. Water Resour Res 34 (10):2573-2585. doi:10.1029/98wr01285

Galloway DL, Jones DR, Ingebritsen SE (eds) (1999) Land Subsidence in the United States U.S. Geological Survey Circular vol 1182. U.S. Geological Survey, Reston, Virginia

Gonzalez de Vallejo L, Ferrer M (2011) Geological Engineering 1edn.,

González PJ, Fernández J (2011a) Drought-driven transient aquifer compaction imaged using multitemporal satellite radar interferometry. Geology. doi:10.1130/g31900.1

González PJ, Fernández J (2011b) Error estimation in multitemporal InSAR deformation time series, with application to Lanzarote, Canary Islands. J Geophys Res 116 (B10):B10404. doi:10.1029/2011jb008412

González PJ, Tiampo KF, Camacho AG, Fernández J (2010) Shallow flank deformation at Cumbre Vieja volcano (Canary Islands): Implications on the stability of steep-sided volcano flanks at oceanic islands. Earth and Planetary Science Letters 297 (3–4):545-557. doi:10.1016/j.epsl.2010.07.006

Guerrero J, Gutiérrez F, Bonachea J, Lucha P (2008) A sinkhole susceptibility zonation based on paleokarst analysis along a stretch of the Madrid–Barcelona high-speed railway built over gypsum- and salt-bearing evaporites (NE Spain). Engineering Geology 102 (1–2):62-73. doi:10.1016/j.enggeo.2008.07.010

Gutiérrez F, Galve J, Lucha P, Bonachea J, Jordá L, Jordá R (2009) Investigation of a large collapse sinkhole affecting a multi-storey building by means of geophysics and the trenching technique (Zaragoza city, NE Spain). Environmental Geology 58 (5):1107-1122. doi:10.1007/s00254-008-1590-8

Hanssen RF (2001) Radar Interferometry. Data Interpretation and Error Analysis, vol 2. Remote Sensing and Digital Image Processing. Springer,

Henderson FM, Lewis AJ (eds) (1998) Principles and Application of Imaging Radar. Manual of Remote Sesnsing, vol 2. John Wiley and Sons, New York, US

Herrera G, Álvarez Fernández MI, Tomás R, González-Nicieza C, López-Sánchez JM, Álvarez Vigil AE (2012) Forensic analysis of buildings affected by mining subsidence based on Differential Interferometry (Part III). Engineering Failure Analysis 24 (0):67-76. doi:10.1016/j.engfailanal.2012.03.003

Herrera G, Fernández JA, Tomás R, Cooksley G, Mulas J (2009a) Advanced interpretation of subsidence in Murcia (SE Spain) using A-DInSAR data – modelling and validation. Nat Hazards Earth Syst Sci 9 (3):647-661. doi:10.5194/nhess-9-647-2009

Herrera G, Tomás R, Lopez-Sanchez JM, Delgado J, Mallorqui JJ, Duque S, Mulas J (2007) Advanced DInSAR analysis on mining areas: La Union case study (Murcia, SE Spain). Engineering Geology 90 (3-4):148-159

Herrera G, Tomás R, Lopez-Sanchez JM, Delgado J, Vicente F, Mulas J, Cooksley G, Sanchez M, Duro J, Arnaud A, Blanco P, Duque S, Mallorqui JJ, De la Vega-Panizo R, Monserrat O (2009b) Validation and comparison of Advanced Differential Interferometry Techniques: Murcia metropolitan area case study. ISPRS Journal of Photogrammetry and Remote Sensing 64 (5):501-512

Herrera G, Tomás R, Monells D, Centolanza G, Mallorquí JJ, Vicente F, Navarro VD, Lopez-Sanchez JM, Sanabria M, Cano M, Mulas J (2010) Analysis of subsidence using TerraSAR-X data: Murcia case study. Engineering Geology 116 (3-4):284-295

Hooper A, Bekaert D, Spaans K, Arıkan M (2012) Recent advances in SAR interferometry time series analysis for measuring crustal deformation. Tectonophysics 514–517 (0):1-13. doi:10.1016/j.tecto.2011.10.013

Jackson JA (1997) Glossary of Geology 4th edn. American Geological Institute, Alexandria, Virginia, US

Kampes BM (2006) Radar Interferometry. Persistent Scatterer Technique, vol 12. Remote Sensing and Digital Image Processing. Springer,

Kappel WM, Yager RM, Todd MS (1999) The Retsof Salt Mine Collapse. In: Galloway DL, Jones DR, Ingebritsen SE (eds) Land Subsidence in the United States, vol 1182. vol US Geological Survey Circular. US Geological Survey, Reston, Virginia, pp 111-120

Lanari R, Casu F, Manzo M, Zeni G, Berardino P, Manunta M, Pepe A (2007) An Overview of the Small BAseline Subset Algorithm: A DInSAR Technique for Surface Deformation Analysis. In: Wolf D, Fernández J (eds) Deformation and Gravity Change: Indicators of Isostasy, Tectonics, Volcanism, and Climate Change. Pageoph Topical Volumes. Birkhäuser Basel, pp 637-661. doi:10.1007/978-3-7643-8417-3_2

López F, Buxó P, Palau J, Marturià J, Concha A, Martínez P (2010) Evaluation of the subsidence and risk of collapse in the estació neighbourhood of the Sallent City (Spain). Paper presented at the Land Subsidence, Associated Hazards and the

Role of Natural Resources Development. Proceedings of EISOLS 2010, Querétaro, Mexico,

Lundgren P, Usai S, Sansosti E, Lanari R, Tesauro M, Fornaro G, Berardino P (2001) Modeling surface deformation observed with synthetic aperture radar interferometry at Campi Flegrei caldera. J Geophys Res 106 (B9):19355-19366. doi:10.1029/2001jb000194

Mancini F, Stecchi F, Zanni M, Gabbianelli G (2009) Monitoring ground subsidence induced by salt mining in the city of Tuzla (Bosnia and Herzegovina). Environmental Geology 58 (2):381-389. doi:10.1007/s00254-008-1597-1

Marturià J, de Diego J, Martínez P, Roca A (2006) Implementation of a subsidence risk management system. Paper presented at the 5th European Congress on Regional Geoscience Cartography and Informations Systems, Barcelona,

Marturia J, Ripoll J, Concha A, Barberà M (2010) Monitoring techniques for analysing subsidence: a basis for implementing an Early Warning System. Paper presented at the Land Subsidence, Associated Hazards and the Role of Natural Resources Development. Proceedings of EISOLS 2010, Querétaro, Mexico,

Massonnet D, Feigl KL (1998) Radar interferometry and its application to changes in the Earth's surface. Rev Geophys 36 (4):441-500. doi:10.1029/97rg03139

Massonnet D, Rossi M, Carmona C, Adragna F, Peltzer G, Feigl K, Rabaute T (1993) The displacement field of the Landers earthquake mapped by radar interferometry. Nature 364 (6433):138-142

Monserrat O (2012) Deformation measurement and monitoring with Ground-Based SAR. Universitat Politècnica de Catalunya, Barcelona

Mora O, Arbiol R, Palà V (2007) The experience of the cartographic Institute of Catalonia (ICC) on continuous DInSAR monitoring of large areas. Paper presented at the Envisat Symposium 2007, Montreux, Switzerland,

Mora O, Mallorqui JJ, Broquetas A (2003) Linear and nonlinear terrain deformation maps from a reduced set of interferometric SAR images. Geoscience and Remote Sensing, IEEE Transactions on 41 (10):2243-2253

Mulas J, Aragón R, Martínez M, Lambán J, García-Aróstegui JL, Fernández-Grillo AI, Hornero J, Rodríguez J, Rodríguez JM (2003) Geotechnical and hydrogeological analysis of land subsidence in Murcia (Spain). Materials and Geoenvironment 50:249-252

Navarro-Sanchez VD, Lopez-Sanchez JM (2012) Improvement of Persistent-Scatterer Interferometry Performance by Means of a Polarimetric Optimization. Geoscience and Remote Sensing Letters, IEEE 9 (4):609-613. doi:10.1109/lgrs.2011.2176715

Navarro-Sanchez VD, Lopez-Sanchez JM, Vicente-Guijalba F (2010) A Contribution of Polarimetry to Satellite Differential SAR Interferometry: Increasing the Number of Pixel Candidates. Geoscience and Remote Sensing Letters, IEEE 7 (2):276-280. doi:10.1109/lgrs.2009.2033013

Oller P, Gonzalez M, Pinyol J, Marturià J, Martínez P (2011) Geohazards Mapping in Catalonia. Journal Torrent, Avalanche, Landslide Rock Fall Engineering 74:8

Palà V, Mora O, Arbiol R, Marturià J (2006) Products derived from an advanced DInSAR-GIS application for risk management. In: ISPRS (ed) Geospatial databases for sustainable development. Goa, India, p 5

Peltzer G, Rosen P (1995) Surface Displacement of the 17 May 1993 Eureka Valley, California, Earthquake Observed by SAR Interferometry. Science 268 (5215):1333-1336. doi:10.1126/science.268.5215.1333

Pipia L, Aguasca A, Fabregas X, Mallorqui JJ, Lopez-Martinez C, Marturia J Mining Induced Subsidence Monitoring in Urban Areas with a Ground-Based SAR. In: Urban Remote Sensing Joint Event, 2007, 11-13 April 2007 2007. pp 1-5. doi:10.1109/urs.2007.371881

Pipia L, Fabregas X, Aguasca A, Duque S, Mallorqui JJ, Lopez-Martinez C Polarimetric Deformation Maps Retrieval of Urban Areas using Ground-Based SAR Acquisitions. In: Geoscience and Remote Sensing Symposium, 2008. IGARSS 2008. IEEE International, 7-11 July 2008 2008. pp IV - 327-IV - 330. doi:10.1109/igarss.2008.4779724

Prati C, Ferretti A, Perissin D (2010) Recent advances on surface ground deformation measurement by means of repeated space-borne SAR observations. Journal of Geodynamics 49 (3–4):161-170. doi:10.1016/j.jog.2009.10.011

Prokopovich NP (1979) Genetic classification on land subsidence. Paper presented at the International Conference on Evaluation and Prediction of Subsidence, Pensacola Beach, Florida,

Pulido-Bosch A, Delgado J, Sola F, Vallejos Á, Vicente F, López-Sánchez JM, Mallorquí JJ (2011) Identification of potential subsidence related to pumping in the Almería basin (SE Spain). Hydrological Processes 26 (5):731-740. doi:10.1002/hyp.8181

Raucoules D, Colesanti C, Carnec C (2007) Use of SAR interferometry for detecting and assessing ground subsidence. Comptes Rendus Geoscience 339 (5):289-302. doi:10.1016/j.crte.2007.02.002

Rodríguez-Estrella T, Manteca JL, García C (2000) Subsidencia minera, en relación con sismotectónica, en La Unión (Murcia). Geotemas 1:150-153

Sansosti E, Casu F, Manzo M, Lanari R (2010) Space-borne radar interferometry techniques for the generation of deformation time series: An advanced tool for Earth's surface displacement analysis. Geophys Res Lett 37 (20):L20305. doi:10.1029/2010gl044379

Schmidt DA, Bürgmann R (2003) Time-dependent land uplift and subsidence in the Santa Clara valley, California, from a large interferometric synthetic aperture radar data set. J Geophys Res 108 (B9):2416. doi:10.1029/2002jb002267

Simons M, Rosen PA (2007) 3.12 - Interferometric Synthetic Aperture Radar Geodesy. In: Editor-in-Chief: Gerald S (ed) Treatise on Geophysics. Elsevier, Amsterdam, pp 391-446

Sousa JJ, Ruiz AM, Hanssen RF, Bastos L, Gil AJ, Galindo-Zaldívar J, Sanz de Galdeano C (2010) PS-InSAR processing methodologies in the detection of field surface deformation—Study of the Granada basin (Central Betic Cordilleras, southern Spain). Journal of Geodynamics 49 (3–4):181-189. doi:http://dx.doi.org/10.1016/j.jog.2009.12.002

Tomás R, García-Barba J, Cano M, Sanabria MP, Ivorra S, Duro J, Herrera G (2012) Subsidence damage assessment of a gothic church using Differential Interferometry and field data. Structural Health Monitoring Accepted, in press

Tomás R, Herrera G, Cooksley G, Mulas J (2011) Persistent Scatterer Interferometry subsidence data exploitation using spatial tools: The Vega Media of the Segura River Basin case study. Journal of Hydrology 400 (3-4):411-428

Tomás R, Herrera G, Delgado J, Lopez-Sanchez JM, Mallorquí JJ, Mulas J (2010a) A ground subsidence study based on DInSAR data: Calibration of soil parameters and subsidence prediction in Murcia City (Spain). Engineering Geology 111 (1-4):19-30

Tomás R, Herrera G, Lopez-Sanchez JM, Vicente F, Cuenca A, Mallorquí JJ (2010b) Study of the land subsidence in Orihuela City (SE Spain) using PSI data: Distribution, evolution and correlation with conditioning and triggering factors. Engineering Geology 115 (1-2):105-121

Tomás R, Lopez-Sanchez JM, Delgado J, Mallorquí JJ, Herrera G (2008) DInSAR monitoring of aquifer compaction due to water withdrawal: Vega Baja and Media of the Segura river (SE, Spain) case study. In: Sánchez JM (ed) Drought: causes, effects and predictions. NOVA publishers, New York, pp 253-276

Tomás R, Lopez-Sanchez JM, Delgado J, Vicente F, Cuenca A, Mallorqui JJ, Blanco P, Duque S DInSAR monitoring of land subsidence in Orihuela City, Spain: Comparison with geotechnical data. In: Geoscience and Remote Sensing Symposium, 2007. IGARSS 2007. IEEE International, 23-28 July 2007 2007. pp 3027-3030

Ulaby FT, Moore RK, Fung AK (1982) Microwave Remote Sensing: Active and Passive. Advanced Book Program. Addison-Wesley, Massachusetts, US

Vieira R, Van Ruymbeke M, Fernández J, Arnoso J, Toro C (1991) The Lanzarote underground laboratory. In: van Ruymbeke M, d'Oreye N (eds) Geodynamical Instrumentation applied to Volcanic Areas, vol 4. Cahiers du Centre Européen de Géodynamique et de Séismologie, Walferdange, Grand-Duchy of Luxembourg, pp 71-86

Waltham T (1989) Ground subsidence. Chapman & Hall, New York, US

Werner C, Wegmuller U, Strozzi T, Wiesmann A Interferometric point target analysis for deformation mapping. In: Geoscience and Remote Sensing Symposium, 2003. IGARSS '03. Proceedings. 2003 IEEE International, 21-25 July 2003 2003. pp 4362-4364 vol.4367. doi:10.1109/igarss.2003.1295516

Wu Y (2003) Mechanism analysis of hazards caused by the interaction between groundwater and geo-environment. Environmental Geology 44 (7):811-819. doi:10.1007/s00254-003-0819-9

Table 1. Radar systems employed in the reported subsidence studies in Spain. ESA: European Space Agency; DLR: German Aerospace Center; JAXA: Japan Aerospace Exploration Agency; UPC: Universidad Politécnica de Cataluña; IG: Institut de Geomàtica; ASI: Italian Space Agency.

Satellite- and ground-based SAR systems	**Agency / Institution**	**Start-End**	**Band**	**Wavelength (cm)**	**Revisiting period (days)**	**Resolution (azimuth x range)**
ERS 1-SAR	ESA	1991-2000	C	5.6	35	4 m x 20 m
ERS 2-SAR	ESA	1995-2010	C	5.6	35	4 m x 20 m
ENVISAT-ASAR	ESA	2002-2011	C	5.6	35	4 m x 20 m
TerraSAR-X	DLR	2007-2012	X	3.1	11	2 m x 3 m
ALOS-PALSAR	JAXA	2005-	L	23.6	46	10 m x 10 m
GBSAR	UPC	2007	X	3.1	User-defined	0.5 m x 0.5 m
	IG	2008-	Ku	1.8	User-defined	0.5 m x 0.0044 rad
Cosmo-Skymed-1	ASI	2007-	X	3.1	< 24 hours	< 1 m x 1 m

Table 2. DInSAR technique and pixel selection criteria implemented in the software packages applied to study subsidence in Spain. Software developer is also indicated.

Technique	**Pixel selection criteria**	**Software name**	**Developer**
Conventional DInSAR	Coherence	DIAPASON (Differential Interferometric Automated Process Applied to Survey Of Nature)	Centre National de la Recherche Scientifique, France
		SARscape	SARMAP, Switzerland
		DORIS (Delft Object-Oriented Radar Interferometry Sotfware)	Technical University of Technology, The Netherlands
		EPSIE	Indra, Spain
Advanced DInSAR	Amplitude	SPN (Stable Point Network)	Altamira Information, Spain
		Delft PSI software	Technical University of Technology, The Netherlands
	Amplitude and coherence	IGPSI (Persistent Scatters Interferometry chain of the Institute of Geomatics)	Instituto de Geomática, Spain
	Coherence	CPT (Coherent Pixel Technique)	Universidad Politécnica de Cataluña, Spain
		DISSIC	Instituto Cartográfico de Cataluña, Spain
		SBAS (Small Baseline)	Institute for Electromagnetic Sensing of the Environment (IREA-CNR.), Italy
		Coherent Target Monitoring	Atlantis Scientific Inc., US.
		Interferometric Stacking	Instituto de Astronomía y Geodesia, Spain
		Multi-Temporal InSAR Analysis Package (MTIANPAC)	Instituto de Astronomía y Geodesia, Spain
	Phase stability	Stanford Method for Persistent Scatterers (StaMPS)	Stanford University, US

Table 3. Estimated precision of subsidence measurements obtained with DInSAR in the analysed areas of Spain (See Figure 1 for locations). (*) The error is computed as the average absolute difference between the in situ and InSAR measurements for the whole available data.

Study site	Field complementary measurements	Period studied	Error (*)
Barcelona (Sant Feliu de Llobregat pilot site)	Levelling	2008-pres.	± 2 mm
Cambrils	Levelling	2008-pres.	± 2 mm
Cardona	GPS	1997-pres.	50 mm
Cardona	Levelling	2006-pres.	± 1.2 mm
Girona	Levelling	2008-2010	± 2 mm
La Palma	GPS	1994-2008	≤ 10 mm
La Unión	Levelling	2003-2004	5.0 ± 3.0 mm
	Extensometers	2003-2010	-
Sabadell-Sant Quirze del Vallès	Levelling	2008-2010	± 2 mm
Sallent	Levelling	1997-2004	< 2 mm / year
	Extensometers	2004-2010	± 0.1 mm
	Inclinometers	2008-2010	0.01 mm / 500 mm
	GB-SAR	2006-2007	
Santa Perpetua de Mogoda	Levelling	2008-pres	± 2 mm
Súria	GPS	2006-2008	12 mm
Tenerife	GPS	1994-2007	≤ 10 mm
Vega Media of the Segura River Basin	Extensometers	2001-2005 2001-2007 2001-2003 2000-2007	5.0 ± 2.8 mm 3.9 ± 3.8 mm < 2.4 mm 4.5 ± 4.1 mm

3 **Table 4.** Comparative of method for measuring ground subsidence. G: Good; MD: Medium; P: Poor; MN: Manually; A: Automatic; SA: Semiautomatic.

Method	Precision	Displacement component	Survey scale	Conditions and operating environment						Degree of automation		Usual sample frequency
				Rural (woody)	*Rural (scrub)*	*Urban*	*Hilly*	*Adverse weather conditions*	*Nocturnal*	*Data acquisition*	*Post-processing*	
Trigonometric levelling	cm	Vertical	Line network	MD-P	MD-P	G-MD	G	P	P	MN	SA	Monthly-annual
Geometric levelling	mm	Vertical	Line network	MD-P	MD-P	G-MD	P	P	P	MN	SA	Monthly-annual
Settlement cell	mm	Vertical	Point	G	G	G	G	MD-G	MD-G	MN-A	MN-SA	Monthly-continuous
Borehole extensometer	mm	Vertical	Point	G	G	G	G	MD-G	MD-G	MN-A	MN-SA	Monthly-continuous
Differential GPS	mm	Vertical and horizontal	Point	MD-P	G-MD	MD-P	G	G-P	G	MN-A	MN-A	Monthly-annual (or continuous)
Conventional DInSAR	mm	Range	Map pixel	P	MD-P	G	G-MD	G	G	A	SA-A	Monthly-weekly (variable)
Advanced DInSAR	mm	Range	Map pixel	MD-P	MD-P	G	G-MD	G	G	A	SA-A	Monthly-weekly (variable)
GBSAR	mm	Range	Map pixel	MD-P	MD-P	G	G	G	G	A	SA-A	Hourly-daily
LIDAR/ALS/ALTM	dm	Range	Map pixel	MD	MD	G	G	MD-P	G-MD	A	SA-A	Monthly-annual

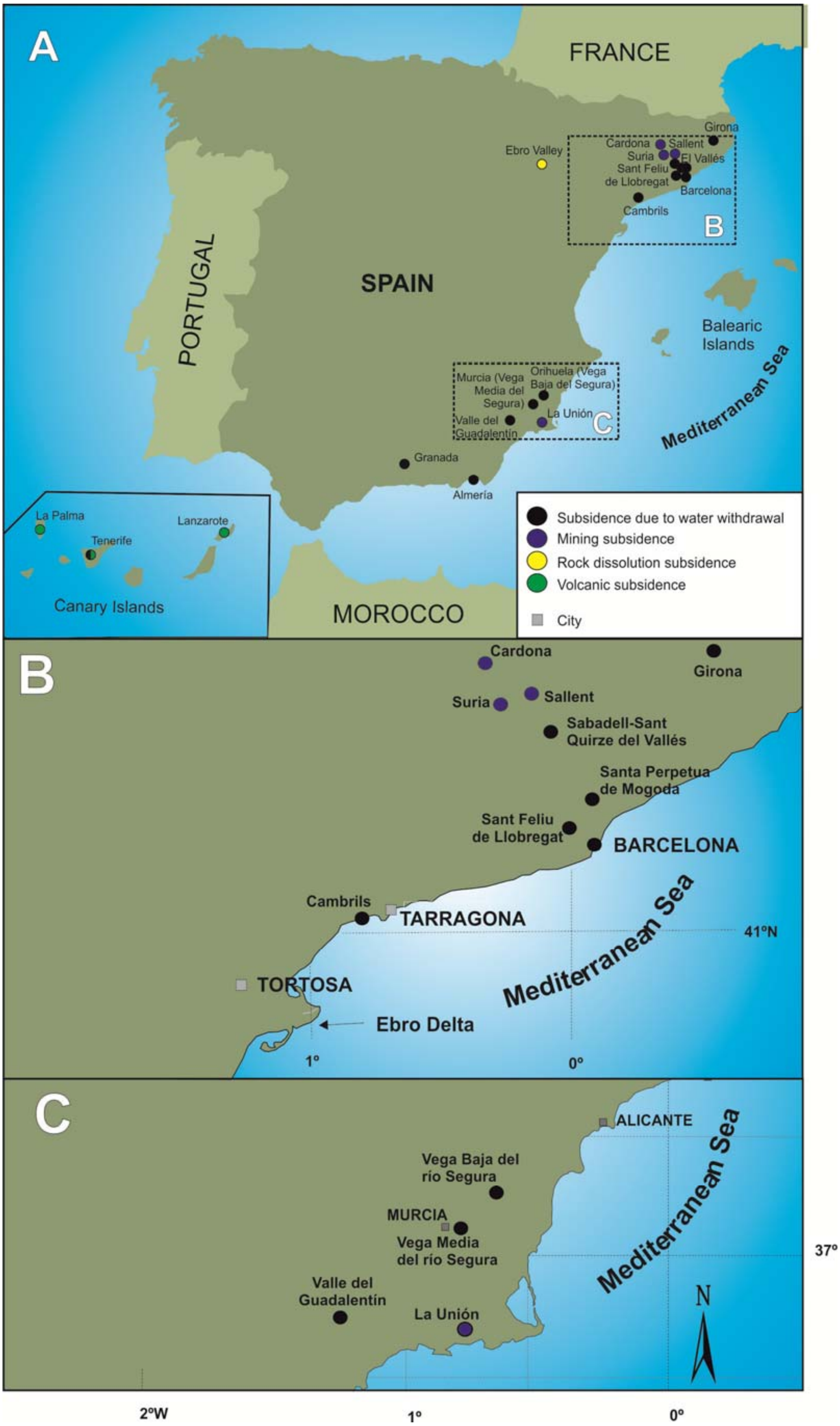
A
FRANCE
Girona
Cardona
Sallent
Suria
El Vallés
Sant Feliu
de Llobregat
Barcelona
Ebro Valley
Cambrils
B
PORTUGAL
SPAIN
Balearic
Islands
Mediterranean Sea
Murcia (Vega
Media del
Segura)
Orihuela (Vega
Baja del Segura)
La Unión
Valle del
Guadalentín
C
Granada
Almería
La Palma
Tenerife
Lanzarote
Canary Islands
MOROCCO
Subsidence due to water withdrawal
Mining subsidence
Rock dissolution subsidence
Volcanic subsidence
City
B
Cardona
Girona
Suria
Sallent
Sabadell-Sant
Quirze del Vallés
Santa Perpetua
de Mogoda
Sant Feliu
de Llobregat
BARCELONA
Cambrils
TARRAGONA
41ºN
TORTOSA
Mediterranean Sea
Ebro Delta
1º
0º
C
ALICANTE
Vega Baja del
río Segura
MURCIA
Vega Media
del río Segura
Valle del
Guadalentín
La Unión
Mediterranean Sea
N
37º
2ºW
1º
0º

Figure 1

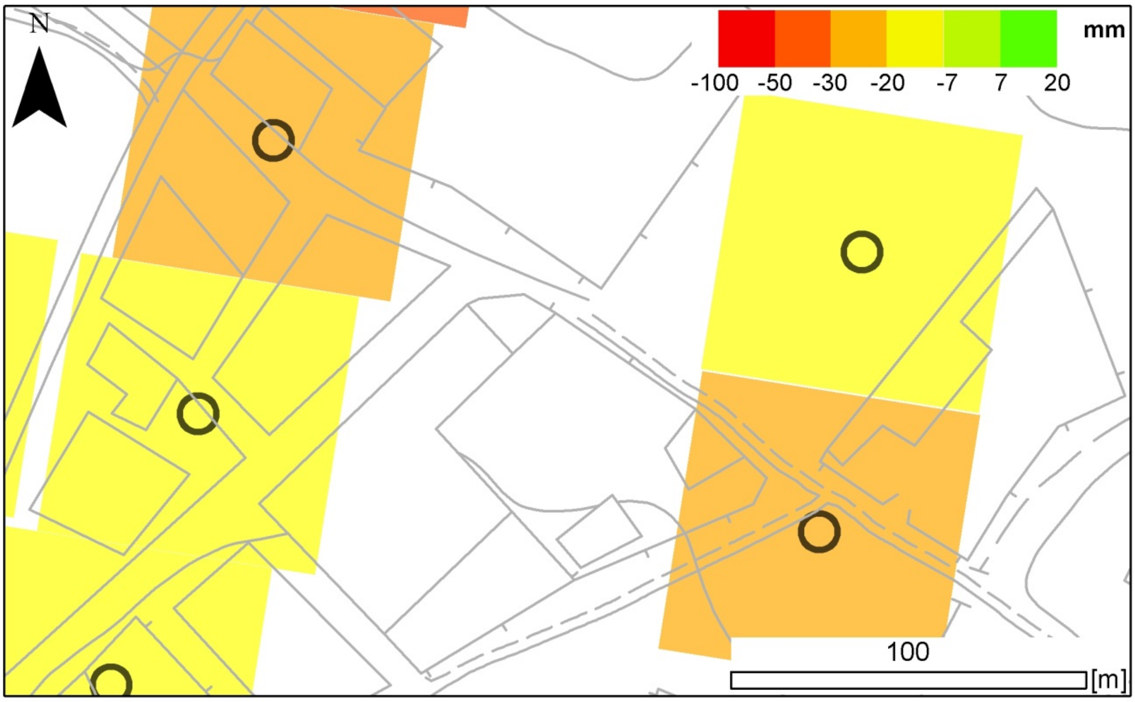

Figure 2

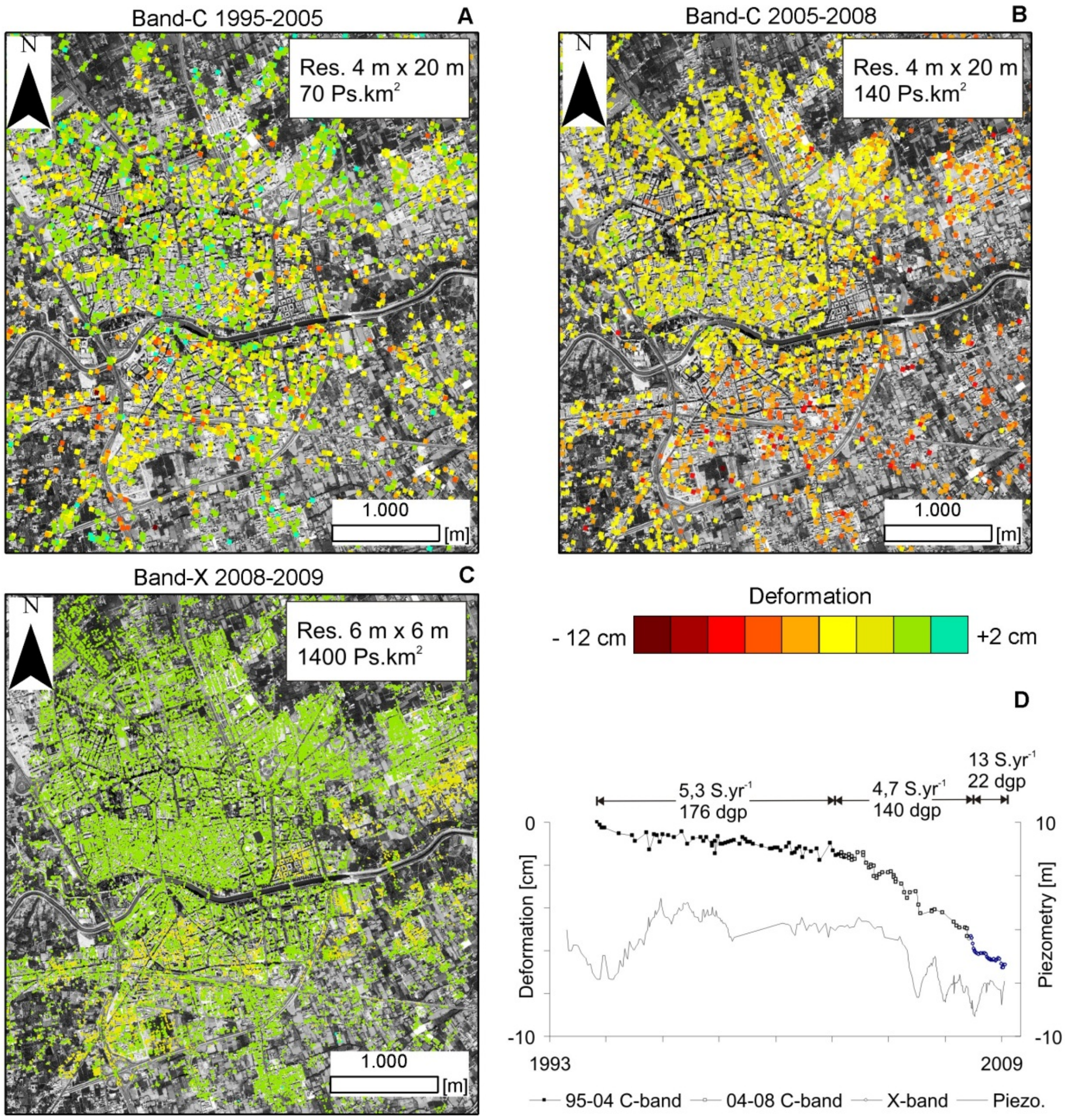

Band-C 1995-2005
A
N
Res. 4 m x 20 m
70 Ps.km^2
1.000
[m]
Band-C 2005-2008
B
N
Res. 4 m x 20 m
140 Ps.km^2
1.000
[m]
Band-X 2008-2009
C
N
Res. 6 m x 6 m
1400 Ps.km^2
1.000
[m]
Deformation
- 12 cm
+2 cm
D
5,3 S.yr^{-1}
176 dgp
4,7 S.yr^{-1}
140 dgp
13 S.yr^{-1}
22 dgp
0
-10
10
-10
Deformation [cm]
Piezometry [m]
1993
2009
95-04 C-band
04-08 C-band
X-band
Piezo.

Figure 3

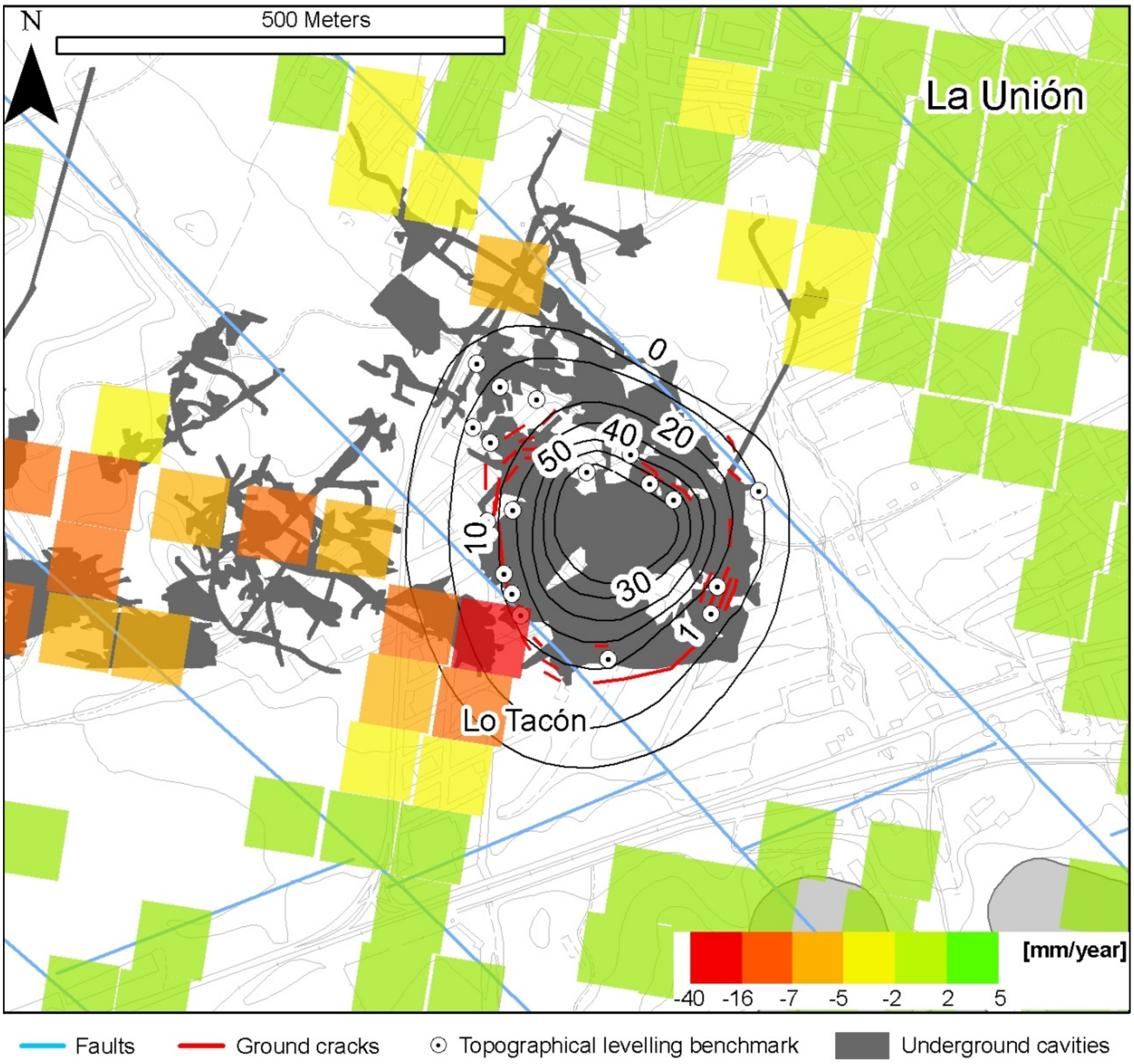
N
500 Meters
La Unión
Lo Tacón
0
10
20
30
40
50
1
[mm/year]
-40 -16 -7 -5 -2 2 5
Faults
Ground cracks
Topographical levelling benchmark
Underground cavities

Figure 4

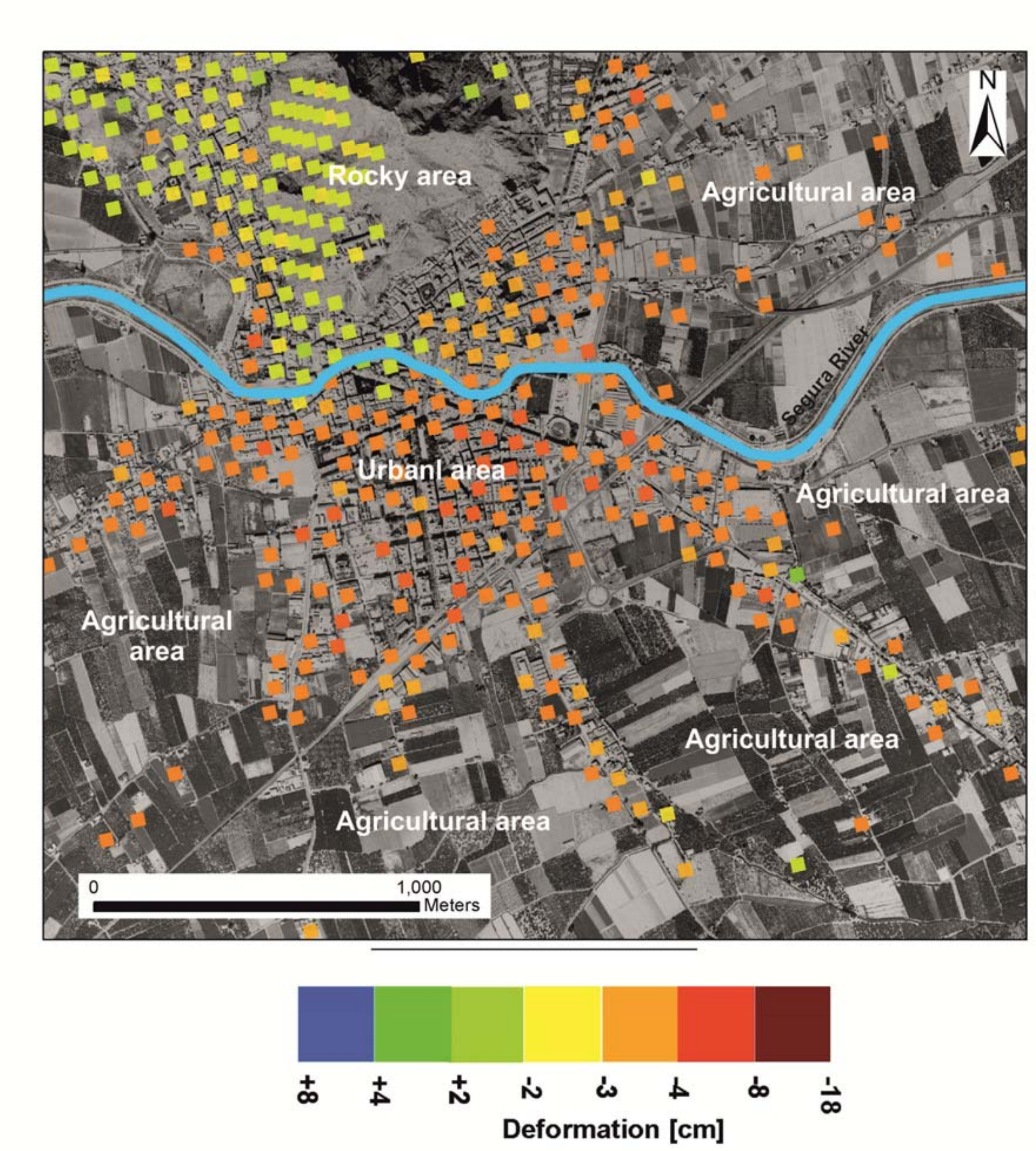
Rocky area
Agricultural area
Segura River
Urbanl area
Agricultural area
Agricultural
area
Agricultural area
Agricultural area
0
1,000
Meters
N
+8
+4
+2
-2
-3
-4
-8
-18
Deformation [cm]

Figure 5

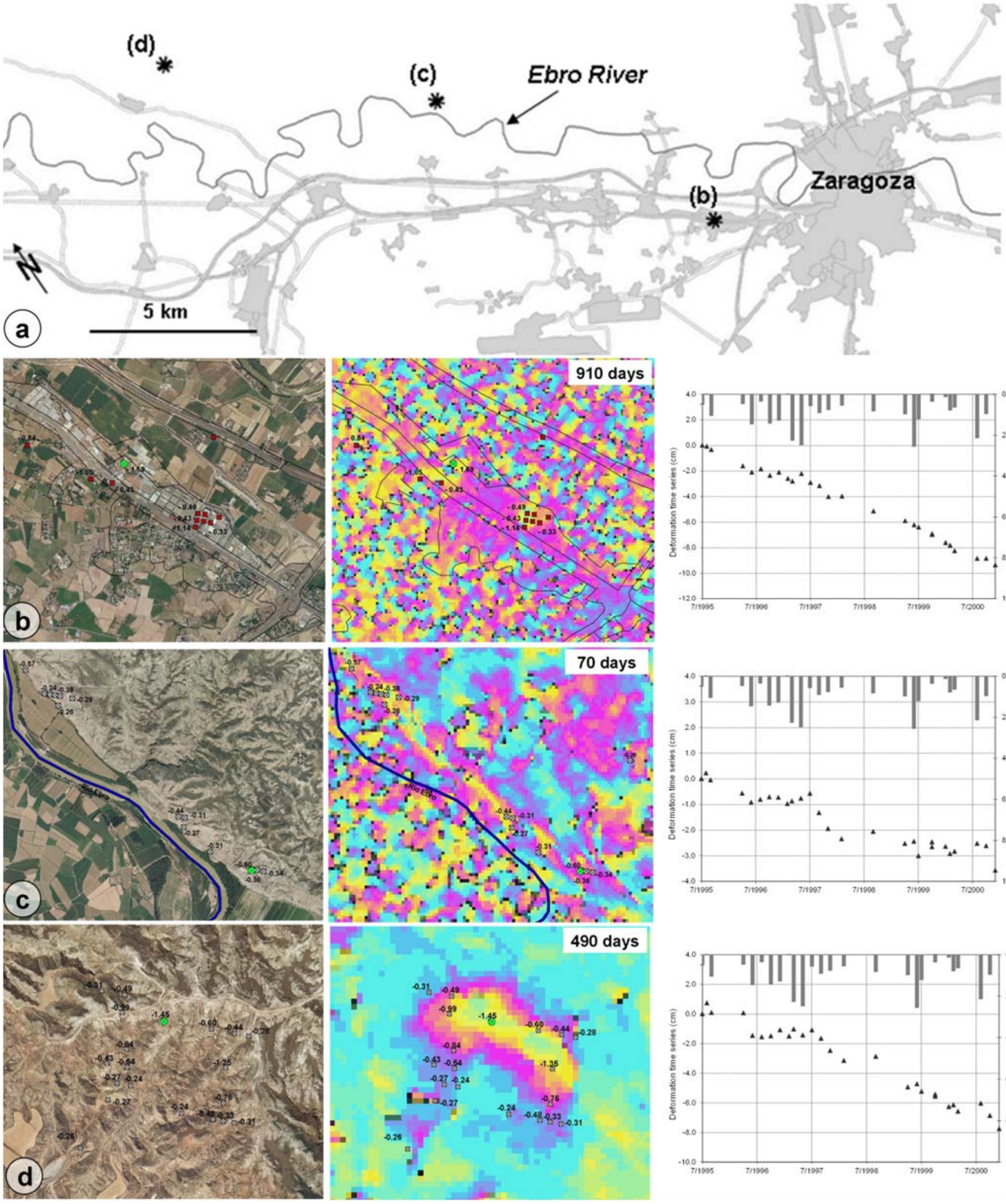

(d)
(c)
Ebro River
(b)
Zaragoza
5 km
a
b
c
d
910 days
70 days
490 days
Deformation time series (cm)
Daily rainfall (mm)
7/1995
7/1996
7/1997
7/1998
7/1999
7/2000

Figure 6

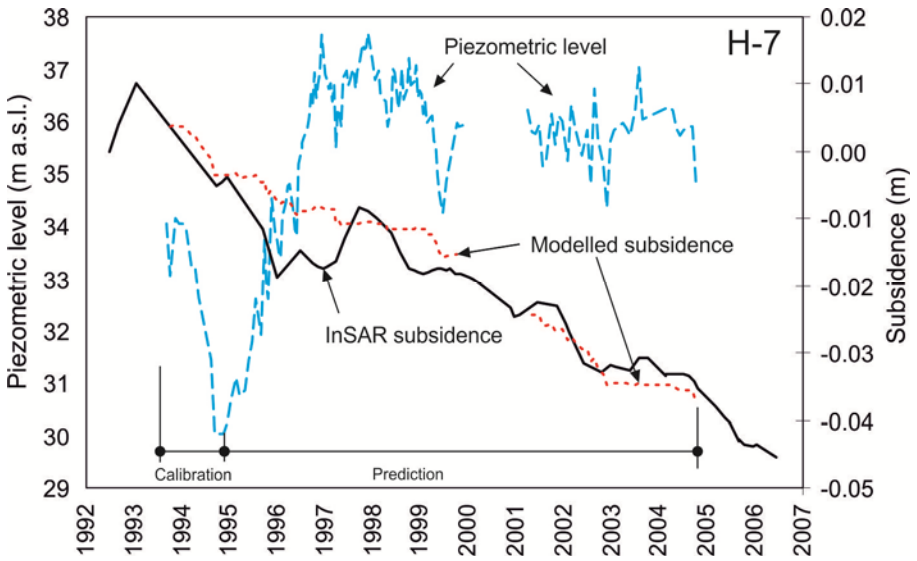
H-7
Piezometric level
Modelled subsidence
InSAR subsidence
Calibration
Prediction
Piezometric level (m a.s.l.)
Subsidence (m)
38
37
36
35
34
33
32
31
30
29
0.02
0.01
0.00
-0.01
-0.02
-0.03
-0.04
-0.05
1992
1993
1994
1995
1996
1997
1998
1999
2000
2001
2002
2003
2004
2005
2006
2007

Figure 7

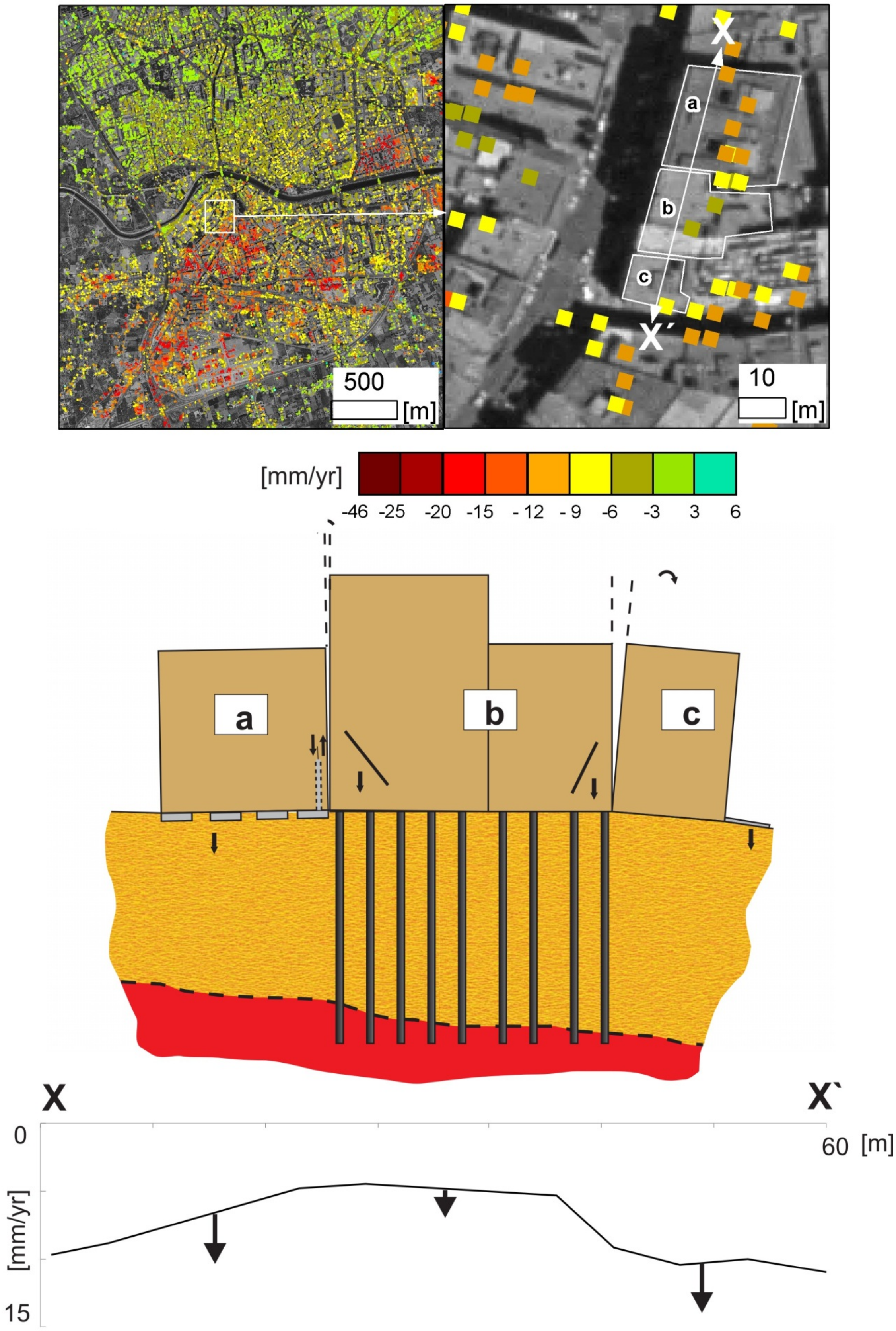

Figure 8

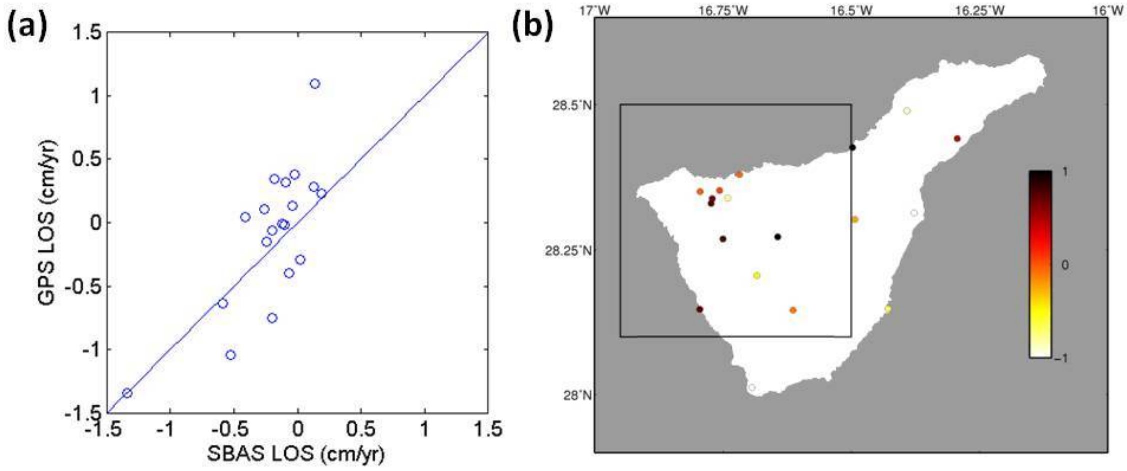
(a)
GPS LOS (cm/yr)
SBAS LOS (cm/yr)
1.5
1
0.5
0
-0.5
-1
-1.5
-1.5
-1
-0.5
0
0.5
1
1.5
(b)
17°W
16.75°W
16.5°W
16.25°W
16°W
28.5°N
28.25°N
28°N
1
0
-1

Figure 9

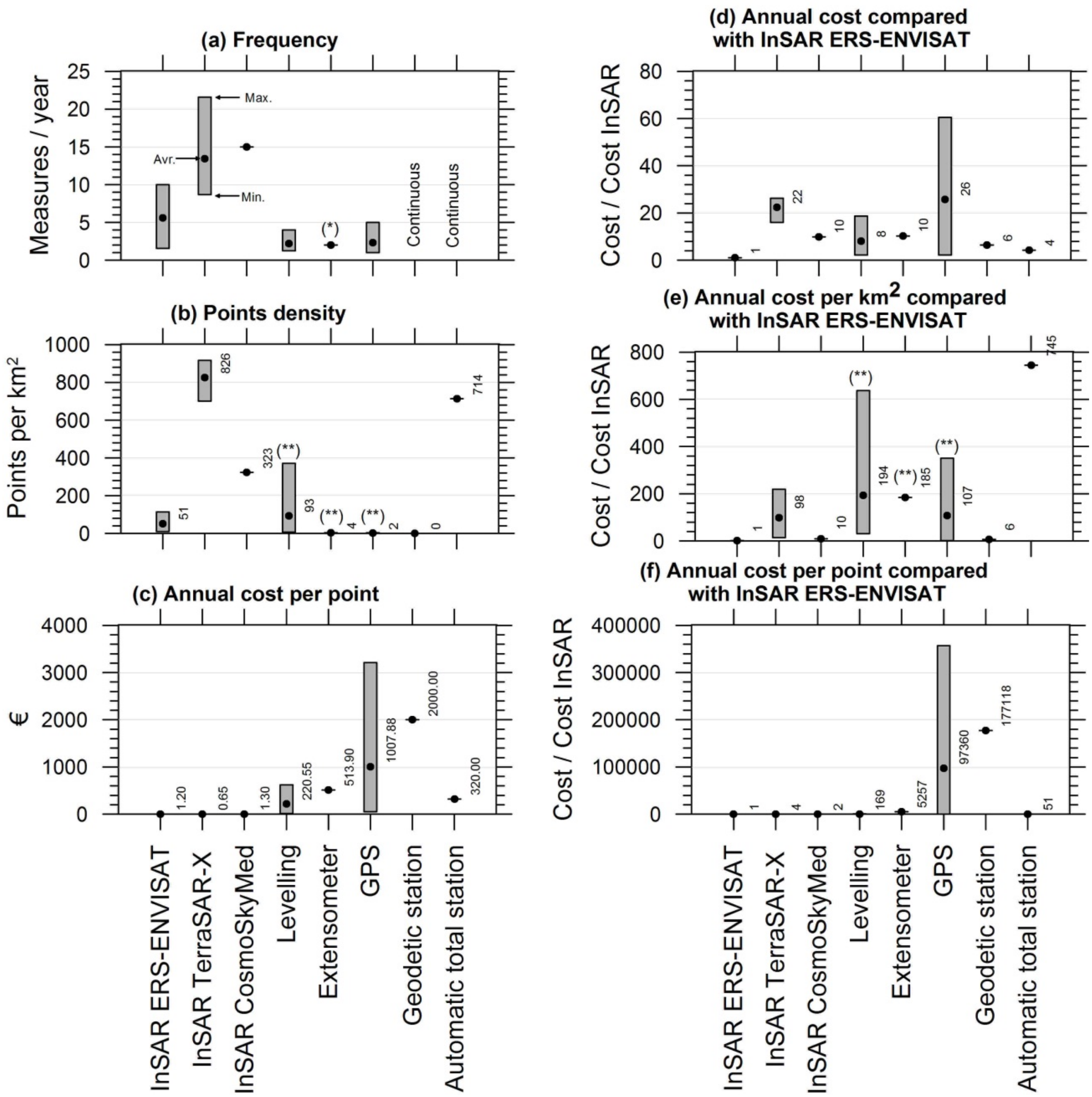
(a) Frequency
Measures / year
Max.
Avr.
Min.
(*)
Continuous
Continuous
(b) Points density
Points per km^2
826
323
(**)
93
51
(**)
4
(**)
2
0
714
(c) Annual cost per point
€
1.20
0.65
1.30
220.55
513.90
1007.88
2000.00
320.00
(d) Annual cost compared with InSAR ERS-ENVISAT
Cost / Cost InSAR
1
22
10
8
10
26
6
4
(e) Annual cost per km^2 compared with InSAR ERS-ENVISAT
Cost / Cost InSAR
1
98
10
(**)
194
(**)
185
(**)
107
6
745
(f) Annual cost per point compared with InSAR ERS-ENVISAT
Cost / Cost InSAR
1
4
2
169
5257
97360
177118
51
InSAR ERS-ENVISAT
InSAR TerraSAR-X
InSAR CosmoSkyMed
Levelling
Extensometer
GPS
Geodetic station
Automatic total station

Figure 10